European Journal of Radiology 114 (2019) 25–31

Contents lists available at ScienceDirect

European Journal of Radiology

journal homepage: www.elsevier.com/locate/ejrad

Research article

Can whole-tumor apparent diffusion coefficient histogram analysis be helpful to evaluate breast phyllode tumor grades?

Yuan Guo[a,1], Wen-Jie Tang[a,1], Qing-cong Kong[b,1], Ying-ying Liang[a], Xiao-rui Han[a], Bing-jie Zheng[c], Lei Sun[d], Xin-hua Wei[a], Zhe Jin[a], Chun-ling Liu[e,*]

[a] Department of Radiology, the Second Affiliated Hospital of South China University of Technology, Guangzhou First People's Hospital, Guangzhou, 510180, China
[b] Department of Radiology, the Third Affiliated Hospital, Sun Yat-Sen University, Guangzhou, 510630, China
[c] Department of Radiology, Henan Cancer Hospital, Affiliated Cancer Hospital of Zhengzhou University, Zhengzhou, 150001, China
[d] School of Biomedical Engineering, Southern Medical University, Guangzhou, 510515, China
[e] Department of Radiology, Guangdong Academy of Medical Sciences/Guangdong General Hospital, Guangzhou, 510180, China

ARTICLE INFO

Keywords:
Breast
Magnetic resonance imaging
Phyllode tumors
Apparent diffusion coefficient (ADC)

ABSTRACT

Purpose: To investigate whether whole-tumor apparent diffusion coefficient (ADC) histogram analysis could be helpful to evaluate breast phyllode tumor (PT) grades.

Materials and methods: This institutional review board-approved retrospective study included 56 PTs (23 benign lesions, 22 borderline lesions, and 11 malignant lesions) from August 2011 to November 2017. MRI was performed using a 1.5 T MR system equipped with a 4-channel SENSE breast coil. All cases were divided into two groups, benign PT (BPT) and borderline or malignant PT (BMPT). The conventional MR parameters included age, longest diameter, shape, margin, internal enhancement characteristics, cystic component of the tumor, wall of the cystic component, peritumoral edema on T2-weighted imaging (T2WI), T1-weighted imaging (T1WI) and T2WI signal intensity, time-signal intensity curve (TIC) patterns and early-stage enhancement ratio (EER). The ADC values were determined in three different types of regions of interest (ROIs), including a circular ROI (ROI-c), single-slice ROI (ROI-s), and whole-tumor ROI (ROI-w). All ADC values were measured twice by Observer A and B (with a 2-week interval). The Ki-67 index was determined, and cases were classified into a "negative group" (Ki-67 < 14%) and a "positive group" (Ki-67 ≥ 14%). SPSS Statistics V21.0 was used for the statistical analyses.

Results: Our study included 23 cases of BPT and 33 cases of BMPT (including 22 borderline PTs and 11 malignant PTs). Only 23 patients in BMPT group had Ki-67 results, and 17 of these were positive. Regarding conventional MR features, significant differences were observed in the margin ($P = 0.011$), cystic component ($P < 0.001$), peritumoral edema on T2WI ($P < 0.001$), and cystic wall ($P = 0.011$) of the PT between the BPT and BMPT groups. Regarding the ADC value, good intraobserver agreement for ROI-c, ROI-s and ROI-w measurements was obtained. For the three different ROIs, the intraclass correlation coefficient (ICC) values were 0.905 for ROI-c ($P > 0.05$), 0.965 ($P > 0.05$) for ROI-s and 0.994 ($P > 0.05$) for ROI-w. ADC parameter indicated that the figure of ROI-s tended to be higher than the ROI-c and ROI-w, while the ROI-c and ROI-w values were similar. However, no significant difference was found in ADC values between the BPT and BMPT groups for ROI-c, ROI-s and mean ROI-w values and the 10th, 25th, 50th and 75th ROI-w. The areas under the ROC curves for the mean ROI-w and the 10th, 25th, 50th and 75th ROI-w were 0.568, 0.613, 0.567, 0.544, and 0.540, respectively.

Conclusion: Based on the results obtained in our study, the whole-tumor ADC histogram could not improve differentiation of the breast PT grade, while conventional MR images could provide more meaningful information, so morphological characteristics may be valuable than ADC value, and ADC could be used as a supplemental method to differentiate PT grades.

* Corresponding author.
E-mail addresses: 10098030@qq.com (Y. Guo), liuchunling79@163.com (C.-l. Liu).
[1] These authors contributed equally to this work.

https://doi.org/10.1016/j.ejrad.2019.02.035
Received 18 January 2019; Received in revised form 12 February 2019; Accepted 26 February 2019

1. Introduction

Phyllode tumors (PTs) of the breast are rare fibroepithelial neoplasms, accounting for 0.3% to 1% of all breast tumors [1,2]. A PT is a biphasic neoplasm characterized by the proliferation of epithelial and stromal components. According to the latest edition of the WHO Classification of Tumors of the Breast published in 2012 [3], PTs are further classified into benign, borderline or malignant subtypes based on stromal cellularity and atypia, mitotic count, stromal overgrowth, and the nature of the tumor borders [4,5]. PTs have a variable risk for local recurrence and distant metastasis. The local recurrence rate ranges from 5% to 30% in benign PTs (BPTs) and from 30% to 65% in borderline and malignant PTs (BMPTs) [6–8], moreover, distant metastasis occurs in up to 22% of malignant PTs [9].

Surgery has been the primary treatment for all subtypes of PTs, however the extent of resection, that is wide local excision or mastectomy and the role of adjuvant radiotherapy and chemotherapy for PT are still debatable [10–13]. The histologic grading of PTs generally correlates with the prognosis; therefore, the ability to grade PTs using diagnostic imaging before surgery is of major benefit to physicians. An accurate preoperative diagnosis of PT is dependent on clinical assessment, imaging analysis and histologic assessment, which will allow appropriate surgical planning. Among mammography, ultrasound and multi-parameter MRI, the latter is known to be useful for differentiating benign and malignant breast tumors and predicting the prognosis because of its multiple qualitative and quantitative parameters [14–18].

Several reports have compared the findings of MRI among different grades of PT; however, literature on the use of multi-parameter MRI, especially the ADC value, for grading of PTs is inconsistent [19–21]. Yabuuchi et al [20] demonstrated significant differences in the ADC value between BPT and BMPT. However, Karashima et al [19] reported no difference between these groups. These conflicting results prompted us to identify a more accurate and quantitative parameter to determine whether the ADC value is helpful in differentiating PT grades [19,22,23].

In recent years, whole-tumor ADC histogram analysis has been widely applied and showed further value in predicting the heterogeneity and aggressiveness of tumors [23,24]. It is well known that breast tumors frequently exhibit biologic heterogeneity; therefore, the commonly used mean ADC, that of a circular ROI, may be limited [22,24,25]. The whole-lesion histogram analysis approach eliminated of the subjectivity inherent in the placement of a focal ROI, resulting in better evaluation of whole tumors [23]. With this new method, compared to a single circular ROI and a single-slice ROI, a whole-tumor volume (WTV) ROI was placed on the entire lesion over contiguous slices, and a histogram of ADC values was constructed with more quantitative information.

Therefore, the purpose of our study was to evaluate ADC parameters acquired by two readers using three different ROI types (circular, single-section and WTV) to determine a suitable ROI type and to investigate whether ADC histogram analysis showed improved predictive value in differentiating PT grades compared to conventional MRI.

2. Materials and methods

2.1. Patients

This retrospective study was approved by our institutional review board. Patients with pathologically confirmed PTs were included in the study. Patients without biopsy or surgery, without MR images acquired after biopsy or surgery, or with MR imaging performed at an outside hospital were excluded from the study (Fig. 1). Finally, 56 patients with PTs who underwent breast MRI from August 2011 to November 2017 were included. The 56 PT patients included 23 benign lesions, 22 borderline lesions, and 11 malignant lesions. All patients underwent surgery after the MRI investigation, and definitive diagnoses were provided by histopathology.

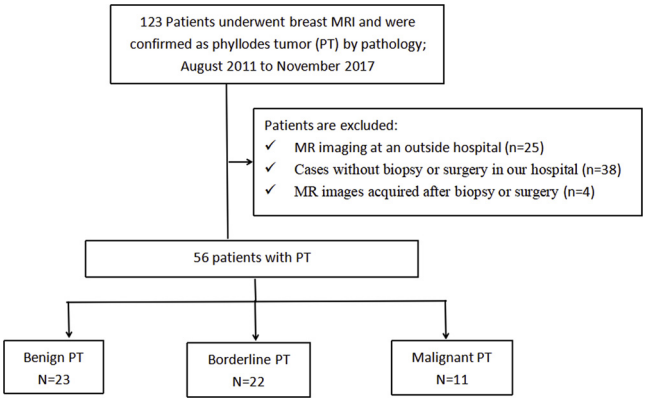

Fig. 1. Flowchart for the case accrual process.

2.2. MRI technique

MRI was performed using a 1.5 T MR system (Achieva 1.5 T, Philips Healthcare, Best, Netherlands) equipped with a 4-channel SENSE breast coil (Invivo Phantom Holder Assy, Galnesville, Florida, U.S.A, Part No: 100,679) with patients in the prone position. Axial T1-weighted images and fat-suppressed T2-weighted images of the breasts were obtained.

The gadolinium-based agent Gd-DTPA (gadopentetate dimeglumine, Magnevist; Bayer Healthcare, Berlin, Germany) was intravenously injected at a dose of 0.2 ml/kg body weight and a rate of 1.5 ml/s, followed by a 20-ml saline flush performed with a high-pressure injector. Axial 3D fat-saturated T1-weighted images were obtained immediately before contrast administration and at 6 consecutive time points (60 s duration each).

Axial DWI with bilateral breast coverage was performed before the administration of Gd-DTPA using single-shot spin-echo echo-planar imaging. The parameters are shown in Table 1.

2.3. Image analysis

The MR images were evaluated independently by two radiologists experienced in breast MRI (Y.G. and W.T., with 11 and 5 years of experience, respectively). All features were determined by consensus. According to the latest Breast Imaging Reporting and Data System (BI-RADS) – MRI, 5th edition [26], the following descriptors were used in the analysis: longest diameter, shape (round, oval or irregular), margin (circumscribed or irregular), and internal enhancement characteristics (heterogeneous or homogeneous). In addition to the BI-RADS MRI descriptors, the following factors were also evaluated: age, lobulation (absence or presence), cystic component in tumor (absence or presence), if present, the wall of the cystic component (irregular or regular), T1-weighted imaging (T1WI) signal intensity (higher or lower than normal breast tissue signal intensity), T2-weighted imaging (T2WI) signal intensity (heterogeneous or homogeneous), peritumoral edema on T2WI, time-signal intensity curve (TIC) patterns on dynamic contrast-enhanced images (persistent pattern (type I), plateau pattern (type II), and washout pattern (type III)), and early-stage enhancement

Table 1
MR acquisition parameter.

Tumor Characteristic	T1WI	T2WI	DWI	CE-MRI
Slice thickness/Gap(mm)	6/1	6/1	6/1	3/0
Repetition time (msec)	4.8	3400	5900	5065
Echo time (msec)	2.1	90	80	66
Field of view (mm^2)	300 × 320	260 × 320	300 × 320	300 × 300
Acquisition time (sec)	78	126	89	394

ratio (EER).

The formula for calculating the EER was as follows: ΔSI = (Sic-SI)/SI × 100%, where Sic is the signal intensity obtained 120 s after contrast medium injection, and SI is the signal intensity obtained before injection.

2.4. Calculation of the ADC value

ADC values were measured on an ADC map by two radiologists (Observer A and Observer B, with 11 and 5 years of experience in imaging, respectively) blinded to the PT group. The ADC values were determined using three methods: (1) circular ROI (ROI-c): placement of circular ROIs on the solid tumor components; the ROI-c was drawn using a circle tool to cover as much of the solid parts of the tumor as possible while avoiding necrotic and cystic or bleeding components; (2) single-slice ROI (ROI-s): the ROI was placed on a single slice of the largest tumor; (3) WTV (ROI-w): the ROI outlined the WTV. To assess the intraobserver agreement, these parameters were measured twice by Observer A and Observer B (with a 2-week interval).

2.5. Pathologic analysis

Patients were diagnosed with a PT according to the WHO Classification of Tumors of the Breast. All cases were divided into two groups, BPT and BMPT. The Ki-67 index was determined and used to classify patients into a “negative group” (Ki-67 < 14%) and a “positive group” (Ki-67 ≥ 14%).

2.6. Statistical analysis

All statistical analyses were performed using a statistical software package (SPSS21.0; SPSS Inc, Chicago, IL, USA). Numerical variance is indicated as the mean and standard deviation. Numerical values were tested for a normal distribution. A Chi-square test and Fisher’s exact probability test were used to compare qualitative parameters; Student’s *t*-test and the Mann-Whitney U test were used to compare quantitative parameters. The intraclass correlation coefficient (ICC) was used to determine the reliability between the two independent radiologists for each parameter; ICC values less than 0.5 are indicative of poor reliability, values between 0.5 and 0.75 indicate moderate reliability, values between 0.75 and 0.9 indicate good reliability, and values greater than 0.90 indicate excellent reliability. ICCs and Bland-Altman plots with 95% limits of agreement were used to determine the intraobserver and interobserver agreement of the ADC. The Kruskal-Wallis rank test was used to compare the differences in ADCs among the three ROI positioning methods. A value of $P < 0.05$ was considered a significant difference.

3. Results

3.1. Histopathological characteristics

Our study included 23 cases of BPT, 22 cases of borderline PT and 11 cases of malignant PT. The patient characteristics and histopathology classification characteristic are shown in Table 2. Only 23 patients in BMPT group had Ki-67 results, and 17 of these were positive.

3.2. Conventional breast MR findings in the BPT and BMPT groups

A comparison of conventional MR findings between the BPT and BMPT groups is presented in Table 3. Significant differences were found in the tumor margin ($P = 0.011$), cystic component ($P < 0.001$), peritumoral edema on T2WI ($P < 0.001$) and the cystic wall of the cystic area ($P = 0.011$) between the BPT and BMPT groups (Figs. 2 and 3.

Table 2
Patient characteristics and Histopathology examination between BPT and BMPT.

Tumor histopathological Characteristic	Benign PT (n = 23)	Borderline PT (n = 22)	Malignant PT (n = 11)
Mitotic activity (per 10 HPF)			
< 5	23	0	0
5-9	**0**	22	0
> 10	0	0	11
Stromal cellularity			
mild	22	9	0
moderate	1	12	1
marked	0	1	10
Stromal atypia			
mild	21	8	0
moderate	2	14	3
marked	0	0	8
Stromal overgrowth			
present	1	6	10
absent	22	16	1
Well-defined margin			
present	23	9	2
absent	0	13	9
Ki-67 status			
NA	23	10	0
Low (< 14%)	NA	4	2
High (≧14%)	NA	8	9

HPF: high-power field; NA: no appliable.

3.3. Comparisons ADC value of three ROIs measurement types between the BPT and BMPT groups

Good agreement was obtained between the observers for ROI-c, ROI-s and ROI-w measurements. For the three ROI methods, the ICC values were 0.905 for ROI-c ($P > 0.05$), 0.965 ($P > 0.05$) for ROI-s and 0.994 ($P > 0.05$) for ROI-w. The Bland-Altman analysis results for intraobserver agreement of ADC parameters among the three different ROI positioning methods are shown in Fig. 4.

ADC parameter indicated that the figure of ROI-s tended to be higher than the ROI-c and ROI-w, while the ROI-c and ROI-w values were similar. However, no significant difference in ADC values was found between the BPT and BMPT groups when using the ROI-c, ROI-s and ROI-w methods and the 10^{th}, 25^{th}, 50^{th} and 75^{th} ROI-w (Table 4). The areas under ROC curves of the mean ROI-w and the 10^{th}, 25^{th}, 50^{th} and 75^{th} ROI-w were 0.568, 0.613, 0.567, 0.544, and 0.540, respectively (Fig. 5). The corresponding cut-off values were 1.781, 1.440, 1.655, 1.793, and 2.034×10^{-3} mm/s^2, respectively.

4. Discussion

In this study, we aimed to evaluate ADC parameters using three different ROI types (circular, single-section and WTV) to determine a suitable ROI type and to investigate whether ADC histogram analysis could improve the predictive value in differentiating PT grades compared to conventional MRI. However, the result of whole-tumor histogram of the ADCs was different than expected; the results may provide indirect proof of the high heterogeneity of PTs.

To the best of our knowledge, only a few studies have investigated associations between imaging findings and tumor grading for PTs before [20], and previous ADC values determined in PTs are controversial. Yabuuchi [20] et al reported that a low ADC value is correlated with a high histologic grade in PTs, although only 10 cases were included in this study. They deduced that a low ADC value in a malignant PT was attributable to stromal hypercellularity. However, a study by Kawashima et al [19] reported no significant difference between BPTs and BMPTs on conventional DWI (15 patients). The results of these two studies appear contradictory. Therefore, we aimed to identify a more

Table 3
conventional MR findings between BPT and BMPT.

MR character	BPT (n = 23)	BM PT (n = 33)	Kvalue	P-value
Age	40.171 ± 10.212	43.451 ± 9.702	−1.219	0.228
Max diameter	44.001 ± 33.389	54.502 ± 35.388	−1.116	0.269
EER (%)	210.111 ± 94.352	220.679 ± 87.191	−0.513	0.610
Shape			−1.369	0.171
Round	2	2		
Oval	21	26		
Irregular	0	5		
Irregular Margin			**−2.528**	**0.011**
Absent	23	25		
present	0	8		
Lobulation			−1.097	0.273
Absent	3	0		
Present	20	33		
Cystic component			**−4.958**	**< 0.001**
Absent	11	6		
Present	12	27	**−2.549**	**0.011**
Irregular wall	4	23		
Regular wall	8	4		
Hyperintense on T_1WI			−1.473	0.141
Absent	23	30		
Present	0	3		
Hyperintense on T_2WI			0.102	0.919
Absent	3	4		
Present	20	29		
Peritumoral edema on T_2WI			−5.270	**< 0.001**
Absent	20	5		
Present	3	28		
Enhancement			−1.004	0.315
Homogeneous	5	5		
Heterogeneous	18	28		
TIC pattern			−1.652	0.099
Type I	5	3		
Type II	18	28		
Type III	0	2		

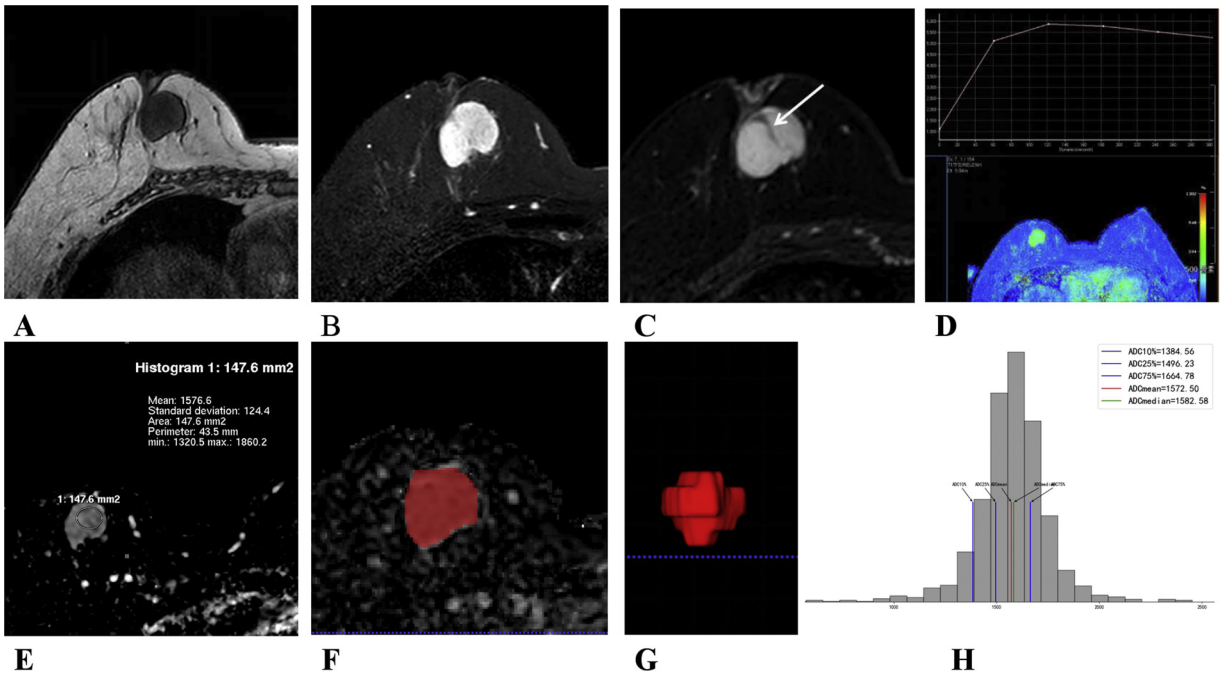

Fig. 2. Benign phyllodes tumor in the right breast of a 52-year-old woman. (A) Transverse non-enhanced T1WI shows a mass with uniform low signal intensity. (B) Transverse fat-saturated T2WI shows the mass with high signal intensity. (C) Transverse high-resolution image obtained after the dynamic study shows homogeneous enhancement. The internal separation (arrow) was also detected. (D) Time-signal intensity curve shows a plateau pattern by contrast-enhanced dynamic imaging. (E) Circle ROI (ROI-c): placement of the circle ROIs on the solid tumor components, and the mean ADC value is 1.576 × 10-3 mm/s2. (F) Single-slice in ROI (ROI-s): placement of ROIs in the single-slice of largest tumor, and the mean ADC value is 1.533 × 10-3 mm/s2. (G) Whole-tumor-volume (ROI-w): placement of ROIs outlining the tumor on the whole tumor volume (WTV). (H) The ADC histogram of the whole tumor volume is shown in Fig. 2H.

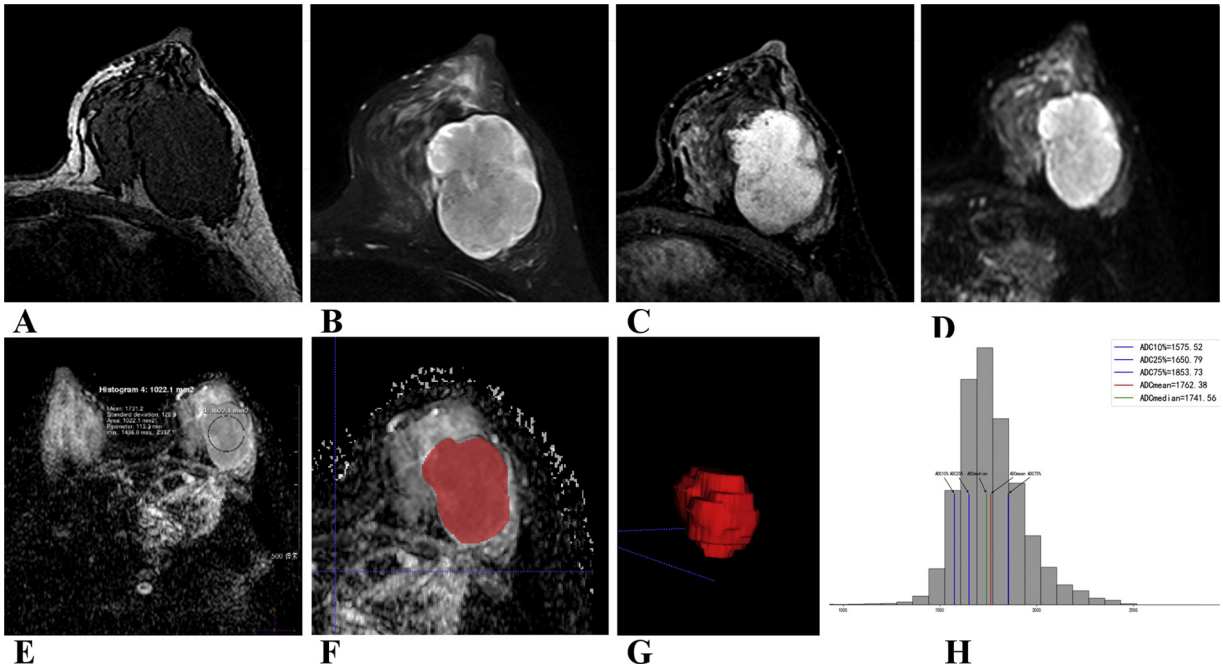

Fig. 3. Borderline phyllodes tumor in the right breast of a 36-year-old woman. (A) Transverse non-enhanced T1WI shows a mass with low signal intensity. (B) Transverse fat-saturated T2WI shows a mass with high signal intensity.(C) Transverse high-resolution image obtained after dynamic study shows heterogeneous enhancement. (D) DWI shows higher signal intensity. (E) Circle ROI (ROI-c): placement of the circle ROIs on the solid tumor components, and the mean ADC value is 1.732 × 10-3 mm/s2. (F) Single-slice in ROI (ROI-s): placement of ROIs in the single-slice of largest tumor, and the mean ADC value is 1.789 × 10-3 mm/s2. (G) Whole-tumor-volume (ROI-w): placement of ROIs outlining the tumor on the whole tumor volume (WTV). (H) The ADC histogram of the whole tumor volume is shown in Fig. 3H.

accurate and quantitative parameter to investigate whether ADC values can be used to differentiate the histological grade of PTs.

In the present study, the ADC values were determined using three methods, ROI-c, ROI-s and ROI-w, to avoid the influence of a limited ROI. Moreover, to obtain good interobserver and intraobserver agreement, two radiologists were blinded to the PT group. Good intraobserver agreement was obtained for ROI-c, ROI-s and ROI-w measurements.

Among the three ROI methods, the ROI-w method contains more information and is more accurate [23,24,27], and ADC histogram results are useful for many tumor types [22,23,28]. However, in our study, the figure of ROI-s tended to be higher than the ROI-c and ROI-w, while the ROI-c and ROI-w values were similar. There are no significant differences were found among the three ROI types. This finding may be due to several reasons. First, the tumors exhibited substantial heterogeneity, which resulted in uncertainty in the proportion of stromal cellularity and epithelium between the BPT and BMPT groups. We assumed that tumor heterogeneity could play a role in imaging features. For example, well, moderately, and poorly differentiated tumors might show similar imaging features. The PT grading system is based on pathology and includes the following parameters: degree of stromal cellularity, stromal atypia, mitosis, stromal overgrowth and tumor margin. However, DWI images and ADC maps are based on the diffusion of water molecules and provide information related to tumor cellularity and tissue composition. Additionally, this pathological classification system does not include parameters such as cell size, extracellular space, and microvessel density, which are known to influence water diffusion [5]. This may explain our negative results regarding associations between tumor grades and ADC values. This can also explain why some authors found significant correlations between ADC values for different PT grades while others did not find correlations. Secondly, the results may be related to the size and internal components of tumors. PTs usually become very large in size, and BMPTs are more likely to have cystic areas. Parsian S et al [29] said that fibroadenomas, which belonged to fibroepithelial neoplasms both with PT, with sparse stroma exhibited higher ADC values and with epithelial hyperplasia exhibited significantly lower ADC values. In our study if necrotic tissue is present in the tumor, it will reduce the average ADC value of the whole volume; however, if some areas are mucinous and have very high ADC values, the average whole-tumor ADC value could be increased. Finally, we assumed that morphological characteristics may be valuable than ADC value, and ADC could be used as a

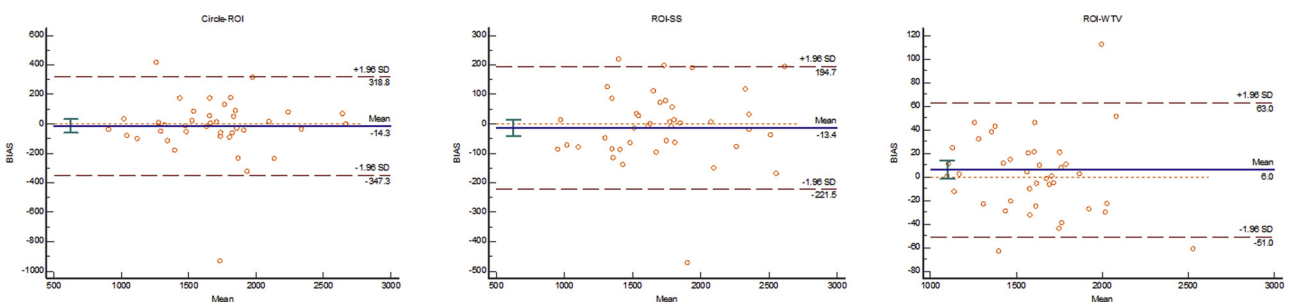

Fig. 4. Interobserver agreement of ADC parameter across three different ROI positioning methods.

Table 4
The result of three methods of ADC measurement between BPT and BMPT.

Tumor Characteristic	BPT (n = 23)	BMPT (n = 33)	Kvalue	P-value
ADC-ROC($\times 10^{-3}$ mm^2/sec)	1.693 ± 0.419	1.671 ± 0.344	0.216	0.830
ADC-SS($\times 10^{-3}$ mm^2/sec)	1.713 ± 0.435	1.726 ± 0.372	0.124	0.902
ADC-WTV($\times 10^{-3}$ mm^2/sec)	1.659 ± 0.313	1.607 ± 0.306	0.607	0.546
10th-ADC-WTV($\times 10^{-3}$ mm^2/sec)	1.334 ± 0.257	1.236 ± 0.268	1.363	0.179
25th-ADC-WTV($\times 10^{-3}$ mm^2/sec)	1.578 ± 0.608	1.429 ± 0.273	1.237	0.221
50th-ADC-WTV($\times 10^{-3}$ mm^2/sec)	1.649 ± 0.309	1.622 ± 0.316	0.316	0.753
75th-ADC-WTV($\times 10^{-3}$ mm^2/sec)	1.811 ± 0.350	1.801 ± 0.383	0.096	0.924

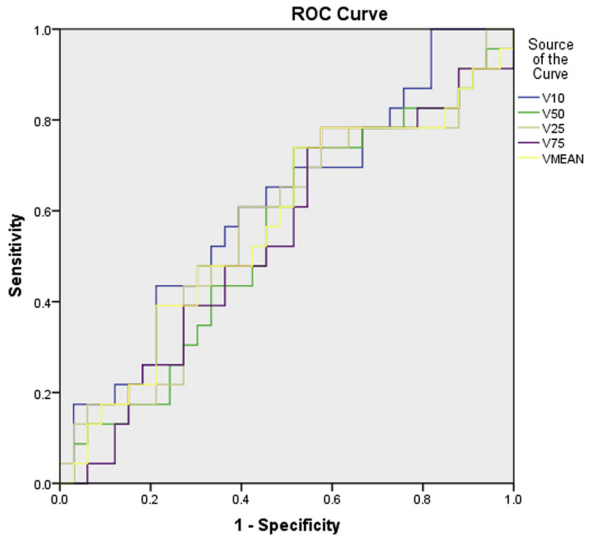

Fig. 5. ROC curve of mean and 10th, 25th, 50th and 75th whole lesion histogram of ADC.

supplemental method to differentiate PT grades, certainly its repeatability and reliability need to be further evaluated and quantified. The ADC is based on water molecule diffusion, but uncertain proportions and arrangements of epithelial tissues and fibers in PTs can cause the absolute ADC value to vary depending on the number of b values, which can affect its accuracy. Thus, for the ADC to be implemented as a method of grading PTs, the reproducibility error needs to be further quantified.

Fortunately, we found that morphological features, including the tumor margin, cystic components, peritumoral edema on T2WI and cyst wall morphology are helpful for differentiating PTs between the BPT and BMPT groups.

For the BMPT group, 8 of 33 (24.2%) cases exhibited blurred and irregular margins, while BPTs all showed well-defined margins in the study. Yabuuchi et al [20] reported that all of the 30 included PTs had smooth margins regardless of whether they were benign or malignant, whereas Tan et al [21] showed that 2 of 9 malignant PTs and 1 of 11 borderline PTs exhibited ill-defined margins on MRI. Though most studies have reported that tumor margins are not correlated with histological grade [15], in our study, irregular margins strongly supported a malignant PT, which indicated the invasive nature of malignant PTs.

Peritumoral edema of PTs is rarely reported and may be correlated with recurrence and the prognosis. Cheon et al reported that peritumoral edema was an independent factor associated with disease recurrence, and the addition of peritumoral edema to the known clinical-pathologic features significantly improved the association with disease recurrence. In our study, peritumoral edema was more likely to appear in BMPTs on T2WI, and the presence of peritumoral edema may be associated with the characteristics of biologically aggressive tumors [30].

Twelve of 23 (52.2%) BPTs exhibited cystic components, and most showed smooth cystic walls (66.7%). However, 27 of 33 (81.8%) BMPTs exhibited cystic components, and the location and shape of cystic areas differed. BMPTs tended to exhibit irregular cystic walls (23/27, 85.2%) more frequently than the BPTs (4/12, 33.3%). Yabuuchi et al [20] reported results similar to ours. Therefore, in our study, the characteristics of the cystic wall were important for differentiating benign from malignant PTs.

With the development of pathology, expression-based and genomics-based classifications of PTs may facilitate diagnosis and grading when used in combination with histologic criteria and may provide clinically useful prognostic information. The genomic landscapes of PTs generated from genomic sequencing provide insights into the molecular pathogenesis of PTs and help to improve the diagnostic accuracy and identify potential drug targets for malignant PTs [5]. 23 patients in the BMPT group had Ki-67 index results, and 17 of these 23 patients had a positive Ki-67 index. This result showed that Ki-67 expression rates are significantly correlated with PT grade [31].

5. Limitations

There are some limitations of our study. This study included a relatively small sample size. Furthermore, more advanced approaches (e.g., intravoxel incoherent motion (IVIM), stretched exponential and/or kurtosis modeling) could be used to extract more valuable biological information from breast DWI scans and may be better diagnostic tools.

6. Conclusion

As demonstrated by our study, after comparing the three different ROI types (circular, single-section and WTV), we found that the whole-tumor ADC histogram could not improve differentiation of the breast PT grade, while conventional MR images provide more meaningful information, so morphological characteristics may be valuable than ADC value, and ADC could be used as a supplemental method to differentiate PT grades. However, further research is needed with more cases.

Disclosure statement

The authors declare that they have no conflict of interest.

Acknowledgement

(1) National Key R&D Program of China (NO. 2017YFC1309100); (2) Medical Scientific Research Foundation of Guangdong Province (No. A2017254); (3) Science and Technology Planning Project of Guangdong Province (No. 2017B020227012); (4) National Natural Science Foundation of China (No. 81771912); (5) Science and Technology Project of Guangdong Province (No.2015B010131011).

References

[1] M.D. Rowell, R.R. Perry, J.G. Hsiu, S.C. Barranco, Phyllodes tumors, Am. J. Surg. 165 (3) (1993) 376–379.

[2] J. Ben Hassouna, T. Damak, A. Gamoudi, R. Chargui, F. Khomsi, S. Mahjoub, M. Slimene, T. Ben Dhiab, M. Hechiche, H. Boussen, K. Rahal, Phyllodes tumors of the breast: a case series of 106 patients, Am. J. Surg. 192 (2) (2006) 141–147.

[3] E.I. Lakhani, S. Schnitt, P. Tan, WHO Classification of Tumours of The Breast, International Agency for Research on Cancer, 2012.

[4] B.Y. Tan, G. Acs, S.K. Apple, S. Badve, I.J. Bleiweiss, E. Brogi, J.P. Calvo, D.J. Dabbs, I.O. Ellis, V. Eusebi, G. Farshid, S.B. Fox, S. Ichihara, S.R. Lakhani, E.A. Rakha, J.S. Reis-Filho, A.L. Richardson, A. Sahin, F.C. Schmitt, S.J. Schnitt, K.P. Siziopikou, F.A. Soares, G.M. Tse, A. Vincent-Salomon, P.H. Tan, Phyllodes tumours of the breast: a consensus review, Histopathology 68 (1) (2016) 5–21.

[5] Y. Zhang, C.G. Kleer, Phyllodes tumor of the breast: histopathologic features, differential diagnosis, and Molecular/Genetic updates, Arch. Pathol. Lab. Med. 140 (7) (2016) 665–671.

[6] A. Moutte, N. Chopin, C. Faure, F. Beurrier, C. Ho Quoc, F. Guinaudeau, I. Treilleux, N. Carrabin, Surgical management of benign and borderline Phyllodes tumors of the breast, Breast J. (2016).

[7] N. Choi, K. Kim, K.H. Shin, Y. Kim, H.G. Moon, W. Park, D.H. Choi, S.S. Kim, S.D. Ahn, T.H. Kim, M. Chun, Y.B. Kim, S. Kim, B.O. Choi, J.H. Kim, Malignant and borderline phyllodes tumors of the breast: a multicenter study of 362 patients (KROG 16-08), Breast Cancer Res. Treat. 171 (2) (2018) 335–344.

[8] A.H. Fathi, M. Julieta Zutel, N.E. Joseph, Giant recurrent phyllodes tumors of the breast: treatment dilemmas and literature review, Breast J. 20 (2) (2014) 210–212.

[9] K.W. Liew, S. Siti Zubaidah, L. Doreen, Malignant phyllodes tumors of the breast: a single institution experience, Med. J. Malaysia 73 (5) (2018) 297–300.

[10] M.I. Liang, B. Ramaswamy, C.C. Patterson, M.T. McKelvey, G. Gordillo, G.J. Nuovo, W.E. Carson, 3rd, Giant breast tumors: surgical management of phyllodes tumors, potential for reconstructive surgery and a review of literature, World J. Surg. Oncol. 6 (2008) 117.

[11] S. Haberer, M. Lae, V. Seegers, J.Y. Pierga, R. Salmon, Y.M. Kirova, R. Dendale, F. Campana, F. Reyal, O. Miranda, A. Fourquet, M.A. Bollet, [Management of malignant phyllodes tumors of the breast: the experience of the Institut Curie], Cancer Radiother. 13 (4) (2009) 305–312.

[12] P. Khosravi-Shahi, Management of non metastatic phyllodes tumors of the breast: review of the literature, Surg. Oncol. 20 (4) (2011) e143–8.

[13] E.O. Onkendi, R.E. Jimenez, G.M. Spears, W.S. Harmsen, K.V. Ballman, T.J. Hieken, Surgical treatment of borderline and malignant phyllodes tumors: the effect of the extent of resection and tumor characteristics on patient outcome, Ann. Surg. Oncol. 21 (10) (2014) 3304–3309.

[14] I. Youn, S.H. Choi, H.J. Moon, M.J. Kim, E.K. Kim, Phyllodes tumors of the breast: ultrasonographic findings and diagnostic performance of ultrasound-guided core needle biopsy, Ultrasound Med. Biol. 39 (6) (2013) 987–992.

[15] T. Kamitani, Y. Matsuo, H. Yabuuchi, N. Fujita, M. Nagao, S. Kawanami, M. Yonezawa, Y. Yamasaki, E. Tokunaga, M. Kubo, H. Yamamoto, H. Honda, Differentiation between benign phyllodes tumors and fibroadenomas of the breast on MR imaging, Eur. J. Radiol. 83 (8) (2014) 1344–1349.

[16] L.J. Li, H. Zeng, B. Ou, B.M. Luo, X.Y. Xiao, W.J. Zhong, X.B. Zhao, Z.Z. Zhao, H.Y. Yang, H. Zhi, Ultrasonic elastography features of phyllodes tumors of the breast: a clinical research, PLoS One 9 (1) (2014) e85257.

[17] L. Duman, N.S. Gezer, P. Balci, C. Altay, I. Basara, M.G. Durak, A.I. Sevinc, Differentiation between Phyllodes tumors and fibroadenomas based on mammographic sonographic and MRI features, Breast Care (Basel) 11 (2) (2016) 123–127.

[18] C. Liu, K. Wang, Q. Chan, Z. Liu, J. Zhang, H. He, S. Zhang, C. Liang, Intravoxel incoherent motion MR imaging for breast lesions: comparison and correlation with pharmacokinetic evaluation from dynamic contrast-enhanced MR imaging, Eur. Radiol. 26 (11) (2016) 3888–3898.

[19] H. Kawashima, T. Miyati, N. Ohno, M. Ohno, M. Inokuchi, H. Ikeda, T. Gabata, Differentiation between phyllodes tumours and fibroadenomas using intravoxel incoherent motion magnetic resonance imaging: comparison with conventional diffusion-weighted imaging, Br. J. Radiol. 91 (1084) (2018) 20170687.

[20] H. Yabuuchi, H. Soeda, Y. Matsuo, T. Okafuji, T. Eguchi, S. Sakai, S. Kuroki, E. Tokunaga, S. Ohno, K. Nishiyama, M. Hatakenaka, H. Honda, Phyllodes tumor of the breast: correlation between MR findings and histologic grade, Radiology 241 (3) (2006) 702–709.

[21] H. Tan, S. Zhang, H. Liu, W. Peng, R. Li, Y. Gu, X. Wang, J. Mao, X. Shen, Imaging findings in phyllodes tumors of the breast, Eur. J. Radiol. 81 (1) (2012) e62–9.

[22] N. Radovic, G. Ivanac, E. Divjak, I. Biondic, A. Bulum, B. Brkljacic, Evaluation of breast Cancer morphology using diffusion-weighted and dynamic contrast-enhanced MRI: intermethod and interobserver agreement, J. Magn. Reson. Imaging (2018).

[23] T. Xie, Q. Zhao, C. Fu, Q. Bai, X. Zhou, L. Li, R. Grimm, L. Liu, Y. Gu, W. Peng, Differentiation of triple-negative breast cancer from other subtypes through whole-tumor histogram analysis on multiparametric MR imaging, Eur. Radiol. (2018).

[24] Y. Guo, Q.C. Kong, Y.Q. Zhu, Z.Z. Liu, L.R. Peng, W.J. Tang, R.M. Yang, J.J. Xie, C.L. Liu, Whole-lesion histogram analysis of the apparent diffusion coefficient: evaluation of the correlation with subtypes of mucinous breast carcinoma, J. Magn. Reson. Imaging 47 (2) (2018) 391–400.

[25] M.H. Choi, S.N. Oh, G.E. Park, D.M. Yeo, S.E. Jung, Dynamic contrast-enhanced MR imaging of the rectum: correlations between single-section and whole-tumor histogram analyses, Diagn. Interv. Imaging 99 (9) (2018) 537–545.

[26] C.C. Morris, C. Lee, ACR BI-RADS® Magnetic Resonance Imaging ACR BI-RADS® Atlas, Breast Imaging Reporting and Data System, American College of Radiology, Reston, VA, 2013.

[27] Y. Wei, F. Gao, M. Wang, Z. Huang, H. Tang, J. Li, Y. Wang, T. Zhang, X. Wei, D. Zheng, B. Song, Intravoxel incoherent motion diffusion-weighted imaging for assessment of histologic grade of hepatocellular carcinoma: comparison of three methods for positioning region of interest, Eur. Radiol. (2018).

[28] R. De Robertis, B. Maris, N. Cardobi, P. Tinazzi Martini, S. Gobbo, P. Capelli, S. Ortolani, S. Cingarlini, S. Paiella, L. Landoni, G. Butturini, P. Regi, A. Scarpa, G. Tortora, M. D'Onofrio, Can histogram analysis of MR images predict aggressiveness in pancreatic neuroendocrine tumors? Eur. Radiol. 28 (6) (2018) 2582–2591.

[29] S. Parsian, N.V. Giannakopoulos, H. Rahbar, M.H. Rendi, X. Chai, S.C. Partridge, Diffusion-weighted imaging reflects variable cellularity and stromal density present in breast fibroadenomas, Clin. Imaging 40 (5) (2016) 1047–1054.

[30] H. Cheon, H.J. Kim, T.H. Kim, H.K. Ryeom, J. Lee, G.C. Kim, J.S. Yuk, W.H. Kim, Invasive breast Cancer: prognostic value of peritumoral edema identified at preoperative MR imaging, Radiology 287 (1) (2018) 68–75.

[31] M.H. Vilela, F.M. de Almeida, G.M. de Paula, N.B. Ribeiro, M.B. Cirqueira, A.L. Silva, M.A. Moreira, Utility of Ki-67, CD10, CD34, p53, CD117, and mast cell content in the differential diagnosis of cellular fibroadenomas and in the classification of phyllodes tumors of the breast, Int. J. Surg. Pathol. 22 (6) (2014) 485–491.